

● *Original Contribution*

VISCOELASTIC AND ANISOTROPIC MECHANICAL PROPERTIES OF IN VIVO MUSCLE TISSUE ASSESSED BY SUPERSONIC SHEAR IMAGING

JEAN-LUC GENNISSON, THOMAS DEFFIEUX, EMILIE MACÉ, GABRIEL MONTALDO,
MATHIAS FINK, and MICKAËL TANTER

Institut Langevin, Laboratoire Ondes et Acoustique, CNRS UMR 7587, ESPCI ParisTech, INSERM ERL U979,
Université Paris VII, Paris, France

(Received 18 August 2009; revised 23 February 2010; in final form 27 February 2010)

Abstract—The *in vivo* assessment of the biomechanical properties of the skeletal muscle is a complex issue because the muscle is an anisotropic, viscoelastic and dynamic medium. In this article, these mechanical properties are characterized for the *brachialis* muscle *in vivo* using a noninvasive ultrasound-based technique. This supersonic shear imaging technique combines an ultra-fast ultrasonic system and the remote generation of transient mechanical forces into tissue via the radiation force of focused ultrasonic beams. Such an ultrasonic radiation force is induced deep within the muscle by a conventional ultrasonic probe and the resulting shear waves are then imaged with the same probe (5 MHz) at an ultra-fast framerate (up to 5000 frames/s). Local tissue velocity maps are obtained with a conventional speckle tracking technique and provide a full movie of the shear wave propagation through the entire muscle. Shear wave group velocities are then estimated using a time of flight algorithm. This approach provides a complete set of quantitative and *in vivo* parameters describing the muscle's mechanical properties as a function of active voluntary contraction as well as passive extension of healthy volunteers. Anisotropic properties are also estimated by tilting the probe head with respects to the main muscular fibers direction. Finally, the dispersion of the shear waves is studied for these different configurations and shear modulus and shear viscosity are quantitatively assessed assuming the viscoelastic Voigt's model. (E-mail: jl.gennisson@espci.fr) © 2010 World Federation for Ultrasound in Medicine & Biology.

Key Words: Muscle tissue, Anisotropy, Viscoelastic, Supersonic shear imaging, Transient elastography.

INTRODUCTION

The biomechanical properties of the skeletal muscle are difficult to assess because this organ is a complex active and passive tissue. The skeletal muscle is composed of muscular fibers running parallel to each other called myocytes. These muscle cells, which are several centimeters long and several tens of micrometers diameter, have both the properties of excitability and contractibility. Each muscle fiber is composed of thousands of sarcomeres, which shorten when an action potential is applied to them. Consequently, the overall response of the fibers to an electrical excitation, natural or artificial, is both a mechanical response in the form of shortening, and a modification of the mechanical properties, in the form of hardening. Some techniques are specifically de-

signed and dedicated to the measurement of functional properties, such as electromyography (EMG), which records the muscle electrical activity (Aminoff 1987), surface mechanomyography (sMMG) (Orizio 1993) or acceleromyography (Viby-Mogensen et al. 2003), which respectively records pressure or acceleration on the skin surface during a contraction. These techniques describe the muscle function through its electrical activity or its mechanical response but have poor spatial resolution. Standard morphologic imaging techniques such as ultrasonography or magnetic resonance imaging (MRI) have also been applied and adapted to image muscle contraction. They follow the morphologic changes of the muscle before and after its shortening with a high spatial resolution but have poor temporal resolution. Recently, the use of ultrasonic ultra-fast imaging combined with electrical stimulation has been shown to allow both good spatial and temporal resolution for the measurement of the muscle mechanical response *in vivo* (Deffieux et al. 2008).

Address correspondence to: Jean-Luc Gennisson, Institut Langevin, Laboratoire Ondes et Acoustique, CNRS UMR 7587, ESPCI Paris Tech, INSERM ERL U979, Université Paris VII, 10 rue Vauquelin, 75231 Paris, Cedex 05, France. E-mail: jl.gennisson@espci.fr

Although the role of viscoelasticity in muscle biomechanics is well recognized, methods for measurements *in situ* are currently limited. Recently, the development of new quantitative elastography techniques has directly studied the modification of the muscle mechanical properties with the contraction. First, magnetic resonance elastography (MRE) has been applied to the measurement of the viscoelastic parameters of *in vivo* muscle. In particular, Dresner et al. (Dresner et al. 2001) have shown the first *in vivo* quantitative measurements of muscle tissue depending on the applied load. They derived a linear model for the relationship between developed strength and muscle stiffness. However, in this study, neither viscosity nor anisotropy are taken into account. In 2003, Gennisson et al. applied transient elastography to the measurements of the muscle stiffness versus developed force (Gennisson et al. 2003). A high anisotropy was observed and a hexagonal model was used for the muscle anisotropy. Using the same transient elastography approach, viscosity estimation was performed on beef muscle as a function of anisotropy (Catheline et al. 2004). These results were conducted with simultaneous recordings of the subjects EMGs (Gennisson et al. 2005). In 2005, Papazoglou et al. conducted the first MRE measurements of muscle stiffness and also demonstrated the high anisotropy of the muscle tissue (Papazoglou et al. 2005). Finally, first MRE clinical trials were conducted in 2007 (Ringleb et al. 2007) on both healthy subjects and patients and significant stiffness difference was exhibited between the two groups. However, in this study, stiffness was only measured along the main muscle direction without taking into account neither anisotropy nor viscosity. In fact, MRE techniques have the advantages of full three-dimensional (3-D) acquisition and can image deep muscles in a well defined and reproducible coordinates system. However, it also suffers limitations since the 3-D acquisition time is not applicable for clinical use (most studies use one-dimensional [1-D] or two-dimensional [2-D] estimation are used to shorten the acquisition time) and deep muscles imaging requires that shear waves generated by an external vibrator reach these deep areas. As a consequence, it limits the access of deep regions to very low frequencies (typically <100 Hz). Finally, the acquisition time and space constraints in the MRI magnet can render the measurements of muscle mechanical properties cumbersome when multiple parameters are to be investigated.

The supersonic shear imaging technique presents a reliable alternative because it measures all these parameters with a freehand and portable system. The main advantages of this approach rely on the fact that the acquisition processing time is very short (<2 s with repeatability), it has minimal contact and space constraints with the muscle through a standard ultrasonic

probe (and, thus, is not interfering with its functioning), it generates plane shear waves which nicely decouple the anisotropic problem along preferred directions and, finally, it gives access to a large spectrum of shear frequencies (100 to 800 Hz) suitable for dispersion measurements and viscoelasticity estimation in a single acquisition. The high interest of the imaging community in the quantification of muscle properties (functional through EMG, or acceleromyography, morphologic through MRI or ultrasonography or mechanical through quantitative elastography techniques) lies in the hope for helping diagnosis or monitoring of the muscle state. Neuromuscular diseases, which are genetic diseases affecting the muscular or nerve function, encompass many different and sometimes rare disorders. Most of them are incurable and can lead to life expectancy less than 25 years. Since a definitive diagnosis is mostly done by a muscle biopsy and protein identification, the pathology identification requires to have a rough idea of what to look for and any kind of information that could help to refine the screening process would greatly help physicians (usually clinical observations, blood testing and electromyography are the main tools). Quantitative elastography might help by providing a parameter that could influence the diagnosis but it could also provide a way to monitor the effectiveness of a treatment by quantifying the changes of the muscle mechanical state. Neuromuscular diseases directly affect proteins, some of them may greatly change the mechanical properties of muscle tissue as is sometimes described by clinicians (Paris and Paris 2001).

Providing a reliable and quantitative tool to estimate muscle mechanical properties could also be useful for rehabilitation and performance training. Whether all these clinical applications could benefit from these measurements is still subject to debate and would need a large amount of clinical trials to be established. We hope that the work undertaken here might pave the way toward such investigations. In this article, we try to present a wide description of the muscle's *in vivo* mechanical properties by using an ultrasound-based quantitative elastography technique known as supersonic shear imaging. We use *in vivo* shear modulus imaging and viscosity estimation to assess and quantify the muscle's mechanical complexity. Moreover, a complete *in vivo* characterization of the biomechanical properties of the biceps brachii (in terms of contraction, extension, anisotropy, elasticity and viscosity) is provided. Shear wave dispersion over a large bandwidth (100–800 Hz) providing quantitative information on shear modulus and shear viscosity are assessed as a function of the muscle contraction level (or developed force), anisotropy (direction of observation) and passive muscle extension (through the elbow's rotation) on five healthy volunteers.

MATERIALS AND METHODS

Five healthy subjects were volunteered for this study. All subjects were informed of the nature of this study and signed an informed consent form submitted to the INSERM ethic committee CQI (Institut National de la Santé et de la Recherche Médicale, Comité de Qualification Institutionnel).

The muscle studied in this study was the *brachialis*. It presents a spatially random distribution of fibers running parallel to one another. This entails the existence of a symmetry axis along the fibers. In the viscoelasticity theory, it has been shown that this kind of symmetry corresponds to a hexagonal system (transverse isotropy) (Zimmer and Cost 1970) and two main axes can thus be defined parallel and perpendicularly to the fibers. Therefore, an experimental homemade set-up was built to characterize muscle elasticity for each main axis. The volunteer upper-arm was then placed in a 90° flexion position as presented in Figure 1. The upper-arm rested on a fixed support. The palm of the subject faced the table and did not move during acquisitions. The angle between the upper-arm and the forearm was set to $\varphi = 90^\circ$. A strap attached the forearm to the dynamometer at wrist level was placed in prone position. The rotation axis of the elbow joint was visually aligned with the perpendicular axis of the dynamometer. Such set-up allows to contract the muscle in an isometric position. The ultrasonic probe was placed at the surface of the biceps brachii and fixed to a rotation axis (θ angle from 0° to 90° with 10° step) to map elasticity with different angle of insonification compared with the muscle fibers main axis. The 0° reference is taken when the probe is parallel to the distal-proximal axis of the arm. It is adjusted on each subject using the real-time ultrasound image. This 0° reference is chosen when the length of hyperechogenic lines is maximal in the B-mode image corresponding to the best alignment of fibers the imaging plane. Before the elasticity mapping, the volunteer was asked to stay at the load instruction ($T \rightarrow$ loading from 0 kg to 5 kg with 1 kg step) for 2 s. A 1-min rest interval was provided between each measurement. Moreover at rest (0 kg loading), the set-up allows the volunteer to extend the arm to characterize the muscle elasticity with the opening angle of the elbow (φ angle from 90° to 165° with 25° step).

Local elasticity measurements were obtained *in vivo* on the *brachialis* muscle using the supersonic shear imaging (SSI) technique (Bercoff *et al.* 2004) with a conventional ultrasonic probe (L7-4, ATL, Seattle, WA, USA) made of 128 elements at 5 MHz central frequency with a 0.3 mm pitch. The probe was driven by an ultrasound research system (V1; Supersonic Imagine, Aix-en-provence, France) made of 128 programmable channels (70 peak-to-peak transmit voltage, 25 kHz

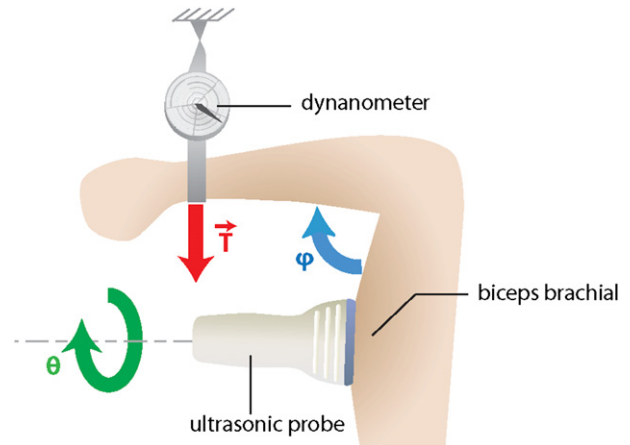


Fig. 1. Top view of the experimental set-up. The volunteer's upper-arm was placed in a 90° flexion position with the palm faced to the table. The angle between the upper-arm and the forearm was set to 90° in a parasagittal plane. A strap attached the forearm to the dynamometer lever arm at the level of the wrist that was placed in a prone position. The rotation axis of the elbow joint was visually aligned with the rotation axis of the dynamometer. Following an isometric contraction of the muscle consisting of increasing the load on the dynamometer ($T \rightarrow$ loading), maps of the biceps brachii and brachialis muscles are then acquired. Then measurements are also achieved with different angles of the elbow (φ angle) without contraction and different position of the probe (θ angle) compared to the main muscle fibers axis.

maximal pulse repetition frequency) and 64 multiplexed received channels (10 bits dynamics, 100 dB time gain amplification).

The *in vivo* SSI mode was described in details in (Tanter *et al.* 2008). It consists of a transient and remote palpation generated by the radiation force induced by a focused ultrasonic beam, the so called “pushing beam”. Each “pushing beam” generates a remote vibration that results in the propagation of a transient shear wave. After generation of this shear wave, an ultra-fast echographic imaging sequence is performed to acquire successive raw radio-frequencies (RF) data at a very high frame rate (up to 20 000 frames/s). Contrary to conventional ultrasonography where an image is achieved using line by line transmit focused beams (typically leading to 50 frames per s), ultra-fast echographic images are achieved by transmitting a single quasi-plane ultrasonic wave in tissues and achieving the beamforming process only in the receive mode. The quasi-plane terminology stands for the fact that the transmitted ultrasonic wavefront is planar in the 2-D imaging plane and slightly diffracting along the probe elevation direction beyond the elevation focal distance. Thus, for ultra-fast imaging, the frame rate is only limited by the time of flight of ultrasonic waves. In this article, the frame rate was set between 2000 and 6000 frames/s depending on the experiment.

Before entering into the SSI mode, the device is functioning as a conventional echographic device (transmit/receive beamforming at 50 frames per s) to accurately place the ultrasonic probe. The operator first asked the volunteer to reach the required load for the experiment and the elastographic sequence was then launched. Then five pushing beams were performed at different locations to explore the whole imaging area with shear waves as previously described in Tanter et al. 2008. For practical clinical configurations, this ultra-short acquisition time prevents the influence of any motion artifacts or natural motions artifacts such as arterial pulse. In this article, two kinds of sequences were used:

- (1) The supersonic shear imaging to generate a full image of the local shear wave velocity (Tanter et al. 2008); and
- (2) The shear wave spectroscopy (SWS) to probe the rheologic properties of the medium by estimating the shear wave dispersion (Defieux et al. 2009)

Supersonic shear imaging sequence

The supersonic shear imaging sequence was slightly adapted from Tanter et al. 2008 with five successive

pushing lines at transducers number 32, 48, 64, 80 and 96 (which correspond to 9.6 mm, 14.4 mm, 19.2 mm, 24 mm and 28.8 mm from the side of the array). Each pushing line consisted of four successive pushing beams at 10, 15 and 20 mm deep of duration 200 μ s. After each one of these five pushing lines, 40 images were acquired in ultra-fast mode at a framerate of 5000 images per s. A low pass filter at 800 Hz was used on the resulting velocity field to improve the signal to noise ratio and limit the effect of the wave dispersion on the measured group velocity. Thanks to a time of flight algorithm, a map of the local shear group velocity was estimated for each of the five pushing lines. The time of flight algorithm is based on cross-correlation between the time profiles of shear displacements at two points located axially at the same depth and laterally distant from four lateral beam widths. No spatial averaging or spatial kernel was introduced for the characterization. Only a 3×3 pixels median filter was done at the end of the signal processing to slightly smooth the final image, which corresponds to a 0.9 mm^2 pixel on the final image. The spatial extent of the shear wave estimate is one ultrasonic wavelength in depth (along the axial direction) and four times the array pitch in the lateral direction. There is no overlap in the axial

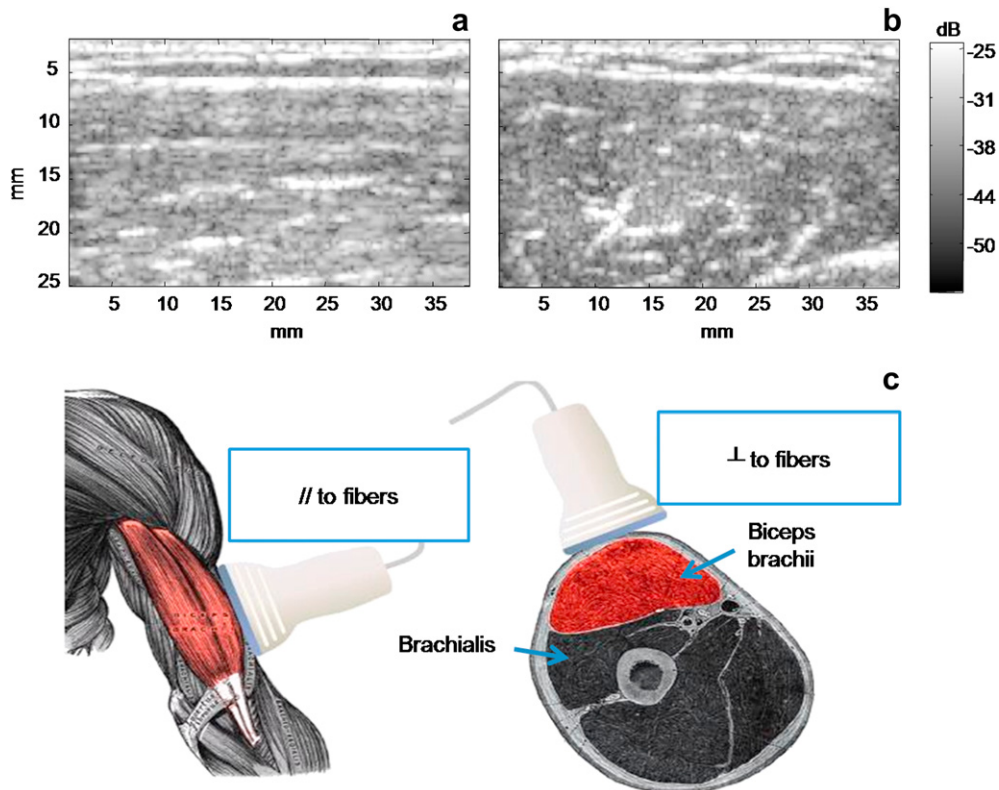


Fig. 2. B-mode image of the upper arm muscles along the fibers (a) and perpendicularly to the fibers (cross section) (b). (c) Anatomical representation the upper arm and of a transverse cross section of the upper arm. Two muscles can be seen, the biceps brachii on top and the brachialis at the bottom.

direction and a three lateral pitches overlap in order to reach the same discretization in the elasticity and ultrasonic image. The five resulting maps corresponding to the five successive excitations are concatenated using a quality factor taking into account several metrics such as ultrasonic correlation coefficient, shear correlation coefficient or signal to noise ratio. From this shear wave group velocity map, it is then possible to compute a shear elasticity map under the assumption of a purely elastic medium as the shear modulus μ can then be written,

$$\mu = \rho \cdot V_g^2, \quad (1)$$

where ρ is the density and V_g is the shear wave group velocity (Royer and Dieulesaint 1996).

The total acquisition for a complete mapping of the muscle elasticity lasted 40 ms (five times 40 frames acquired with a 5000 Hz framerate). So for practical clinical configurations, this ultra-short acquisition time will prevent the influence of any motion artifacts or natural motions artifacts. Considering the energy deposit, in the worst case scenario where we consider all pushing beams to be at the same location, the total pushing time was found to be 3 ms. This leads to an ISPTA (intensity spatial-peak temporal-average) of 400 mW/cm^2 for a one second pause after each acquisition, a value far below the 720 mW/cm^2 level recommended by the FDA. From each acquired map, a $10 \times 10 \text{ mm}^2$ region-of-interest (ROI) was defined in the *brachialis* to extract the mean group velocity and compare it for different sets of parameters (anisotropy, level of contraction, elbow flexion). The standard deviation in this ROI was used as an estimate of the quality of the measure. The influences of

the contraction level on the shear wave group velocity were investigated on five healthy volunteers.

Shear wave spectroscopy sequence

The SWS sequence, dedicated to the measurement of the shear wave dispersion (phase velocity versus frequency), corresponds to the sequence proposed in Deffieux *et al.* 2009. This technique is based on the super-sonic shear imaging and it determines the shear wave phase velocity between 50 and 1800 Hz in the best cases. A Fourier transform is performed on the shear wave velocity movie to have access to the shear wave phases for each frequency of the bandwidth. Then phases are linearly fitted to get the shear wave velocity dispersion curve. In Deffieux *et al.* 2009, to improve the overall quality of the measurement, 10 successive acquisitions were averaged. Here, only one $200 \mu\text{s}$ pushing beam per pushing line was used to limit the energy deposit strictly to the probed area. The ROI, a 10 mm long and 5 mm high box, was set in the *brachialis* muscle, approximately 20 mm deep below the skin. The position of the first pushing beam was automatically set from the position of this ROI. Considering the energy deposit, the total pushing time was found to be 2 ms leading to an ISPTA of 266 mW/cm^2 for a 1 s pause after each acquisition, again far below the FDA recommendation of 720 mW/cm^2 . The SWS sequence was repeated 10 times to investigate the repeatability of the results with a 2 s pause between each acquisition. The Voigt's model, which has been used extensively to characterize the muscle viscoelastic properties (Fung 1981), describes the mechanic behavior of a medium as a parallel arrangement of a spring of elasticity (shear modulus) μ and a dashpot of viscosity η , thus,

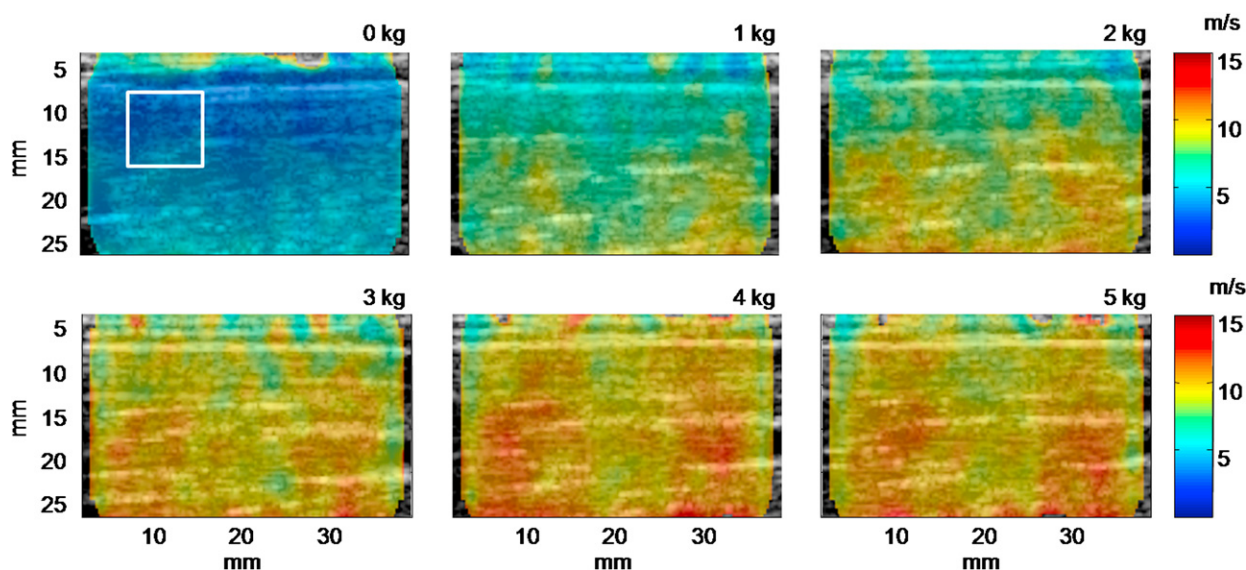


Fig. 3. Shear wave maps of the biceps brachii and brachialis muscles as a function of the load from $T = 0$ to 5 kg along the fiber // (longitudinal). Volunteer no. 1 is placed in prone position with an $\varphi = 90^\circ$ angle of the elbow.

linking the applied strain σ to the resulting deformation ϵ with the well known equation:

$$\sigma = \mu\epsilon + \eta\partial\epsilon, \tag{2}$$

Under the assumption of plane shear wave propagation both perpendicular and parallel to the fibers, this governing equation leads to the derivation of two decoupled wave equations for shear waves in a transverse isotropic medium and the expression of the phase velocity for each propagation direction can be written as (Chen et al. 2004):

$$V_\phi(\omega) = \sqrt{\frac{2(\mu^2 + \omega^2\eta^2)}{\rho(\mu + \sqrt{\mu^2 + \omega^2\eta^2})}}. \tag{3}$$

The Voigt model thus allows to link the shear modulus μ and viscosity η to the dispersion law of the medium $V_\phi(\omega)$. Thanks to a non linear optimization technique, such as the classical Nelder-Mead technique (Nelder and Mead 1965), it is possible to estimate both μ and η , from the measurement of the dispersion law $V_\phi(\omega)$. Using these techniques, for each orientation of the probe compared to the main axis of the muscle fibers (in the following, along the fibers is notified by the symbol // and perpendicularly is notified by the symbol \perp) three experiments were tested: The influence of loading on the elasticity of the muscle for five different volunteers in term of global elasticity and dispersive medium; the elastic anisotropic properties of the *brachialis* muscle and the impact of the passive extension of the *brachialis* muscle on the elastic properties.

RESULTS

Typical B-mode images are presented in Figure 2 along the muscle fibers (Fig. 2a) and perpendicularly to the muscle fibers (Fig. 2b). In Figure 2c, an anatomical representation of the upper arm is presented. One can notice the presence of two main muscles, the biceps under the skin and the brachialis deep below. These two muscles are presented on the B-mode images (Fig. 2a and b). For both configurations the influence of the contraction level on the elasticity was assessed.

Mapping of shear wave group velocity during isometric contraction

The first experiment was made on volunteer no. 1 for different loads (from $T = 0$ kg to 5 kg with 1 kg step). Elasticity maps were acquired for two different axis of insonification in the muscle, along the fibers (Fig. 3) and perpendicularly to the fibers (Fig. 4). An increase of the global elasticity of both muscles is clearly visible in both configurations (from 4.0 to 36.6 kPa // and from 2.3 to 4.0 kPa \perp in shear modulus under the assumption of a purely elastic model). Moreover, the elasticity contrast between the biceps and the brachialis increases strongly with contraction when measured along the fibers (Fig. 3) but gently when measured perpendicularly to the fibers (Fig. 4). Biceps and brachialis muscles can, thus, be separated in terms of the change in elasticity with the contraction. With no contraction, the biceps brachii, softer than the brachialis when measured along the fibers, is harder than the brachialis when measured perpendicularly to the fibers.

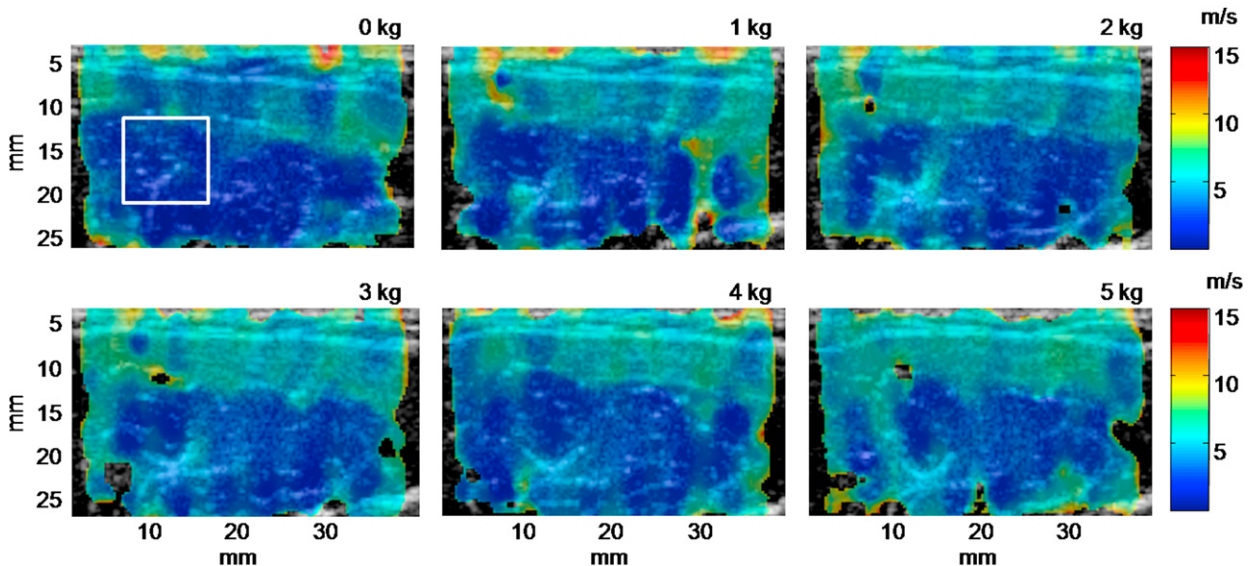


Fig. 4. Shear velocity maps of the biceps brachii and brachialis as a function of the load from $T = 0$ to 5 kg measured perpendicularly to the fibers \perp (transverse). Volunteer no. 1 is placed in prone position with a $\theta = 90^\circ$ angle of the elbow. The two muscles biceps brachii (the biceps [upper part], the brachialis [lower part]) are easily distinguishable in terms of shear wave speed.

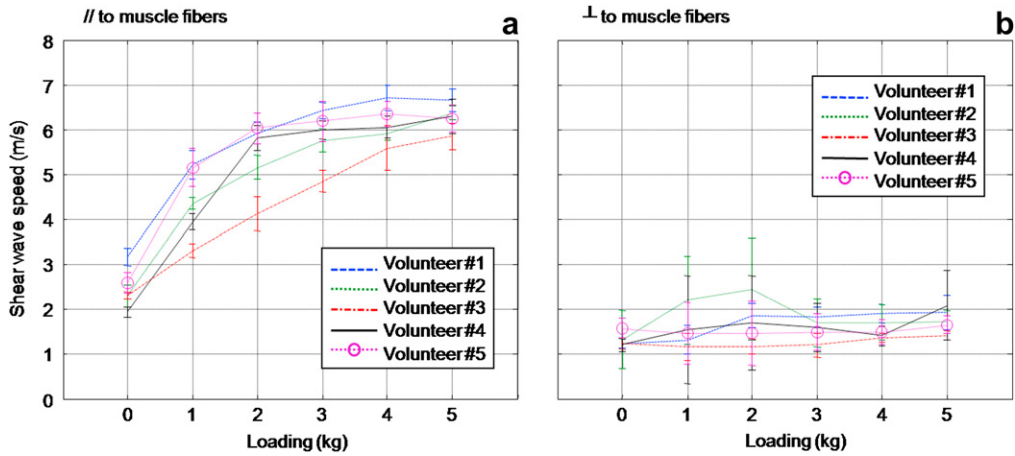


Fig. 5. Mean shear wave group velocity over the ROI brachialis along (a) and perpendicularly (b) to the muscle fibers as a function of the load from $T = 0$ to 5 kg for 5 healthy volunteers.

These contraction experiments were performed on the five healthy volunteers with the same instructions of loading from $T = 0$ kg to $T = 5$ kg for each volunteer. In Figure 5 is presented the mean shear velocity in the ROI defined in Figures 3 and 4 where error bars correspond to the standard deviation inside these ROI. Shear wave group velocity vs. load curves follow the same law for each volunteer and is presented for both positioning of the probe along (Fig. 5a) and perpendicularly (Fig. 5b) to the fibers. Along the fibers, the shear wave group velocity increases and reaches a plateau; when measured perpendicularly to the muscle fibers, the shear wave group velocity increases slowly and quasi-linearly.

Shear wave group velocity and anisotropy

Anisotropic properties measured on volunteer no. 1 are shown in Figure 6 where shear wave group velocity is plotted as a function of the angle θ between the probe and the main axis of the muscle fibers for two different loads (0 kg and 3 kg). For $\theta = 0^\circ$, corresponding to a propagation of the shear wave along the fibers, the shear wave group velocity is three times higher for a $T = 3$ kg loading than at rest. For $\theta = 90^\circ$, corresponding to a propagation of the shear wave perpendicularly to the muscle fibers, the shear wave group velocity is barely higher at rest than for a $T = 3$ kg loading. In between those two main axes ($\theta = 0^\circ$ and $\theta = 90^\circ$) the shear wave group velocity increase for both loads, result that is in good agreement with the literature (Genisson *et al.* 2003). However, one can notice that anisotropy is more visible in the contracted state that in the rest state. Each intermediate position of the probe corresponds to a mix of the elastic properties parallel and perpendicular to the fibers.

Shear wave dispersion and contraction

Shear wave phase velocity is presented in Figure 7 for different loads on volunteer no. 1 along (Fig. 7a) and perpendicularly (Fig. 7b) to the muscle fibers. Similarly to shear wave group velocity measurements, the shear wave phase velocity increases with the load for all frequencies. More precisely, the shear wave phase velocity only increases slightly with respect to frequency and for each load tested, the medium can be considered as non-dispersive when probed along the fibers. Perpendicularly to the fibers, the shear wave phase velocity increases

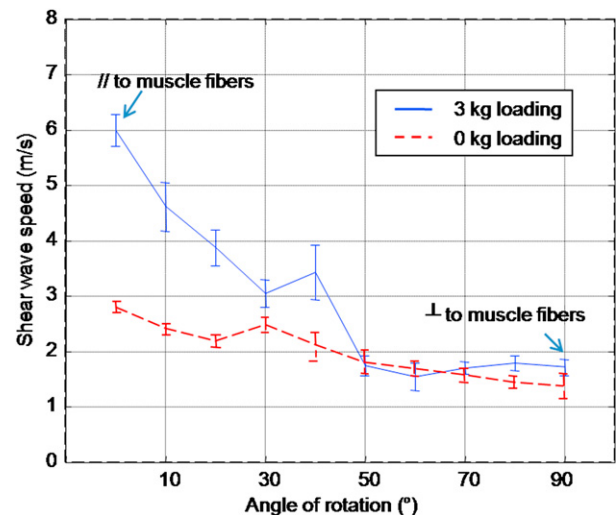


Fig. 6. Shear wave group velocity as a function of the angle of rotation θ between the ultrasonic probe and the muscle fibers. $\theta = 90^\circ$ corresponds to the probe perpendicularly to the fibers and $\theta = 0^\circ$ corresponds to the probe placed along the fibers. Two levels of contraction are presented $T = 0$ kg (blue solid curve) and $T = 3$ kg (red dashed curve). The errorbars correspond to the standard deviation over the whole elastic map for each angle of rotation.

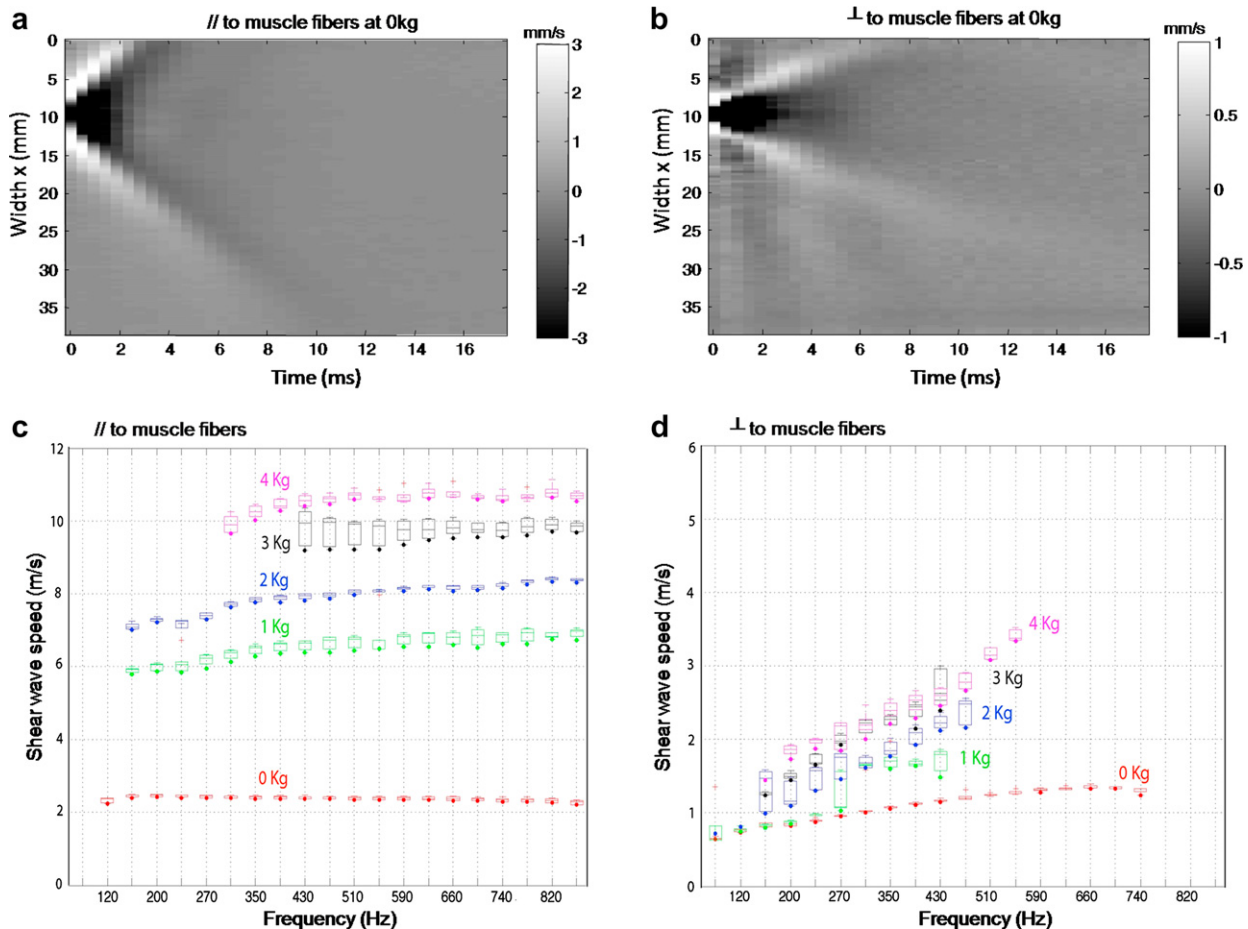


Fig. 7. Velocity field of the shear wave velocity along the fibers (a) and perpendicularly to the fibers (b) at 0 kg contraction. Shear wave phase velocity along the fibers (c) and perpendicularly to the fibers (d) for volunteer no. 1 as a function of the frequency for different loads (from 0 to 5 kg). Along the fibers the brachialis is non dispersive and *a contrario* perpendicularly the muscle is dispersive with an increasing slope from 2 to 10 mm.

strongly with respect to frequency and the slopes of the dispersion curves increase with the contraction.

Using dispersion curves and the Voigt's model, elasticity and viscosity can be deduced from eqn (3). Results are presented in Figure 8 and summarized in Table 1. Both elasticity (μ) and viscosity (η) increase with the contraction level. Nevertheless, one can notice that, for an increasing loading, elasticity grows much faster than perpendicularly to the muscle fibers. As expected, high dispersion in the shear waves velocity curves leads to higher viscosity values. Moreover, the higher the elasticity is and the larger the effect of the dispersion on the viscosity values is.

Muscle passive extension

The passive extension of the biceps was investigated in term of shear wave group velocity. Volunteer no. 1 was asked to be at rest and the elbow was passively opened from $\varphi = 90^\circ$ to 165° with 25° step. For each

positioning of the arm a shear wave group velocity map was acquired as presented in Figure 9. Along the fiber the global shear wave group velocity increases strongly (from 2.7 m/s to 5.7 m/s in the *brachialis*) and the maps remains homogeneous, whereas shear wave group velocity increases very slowly (from 1.2 to 1.8 m/s in the *brachialis*) with heterogeneous maps perpendicularly to the fibers. In fact, one can notice that the biceps and the brachialis have different shear wave group velocity when measured perpendicularly to the fibers (2.3 m/s in the biceps vs. 1.2 m/s in the brachialis for $\varphi = 90^\circ$). In this direction, the passive extension does not affect much the shear wave group velocity in both muscles (2.3 to 2.5 m/s in the biceps and 1.2 to 1.8 m/s in the brachialis).

On Table 2 and Figure 10 are presented results of the shear wave group velocity for the two ROIs defined in Figure 9 (ROI no. 1 is defined in the biceps brachii and ROI no. 2 is defined in the brachialis). Those values

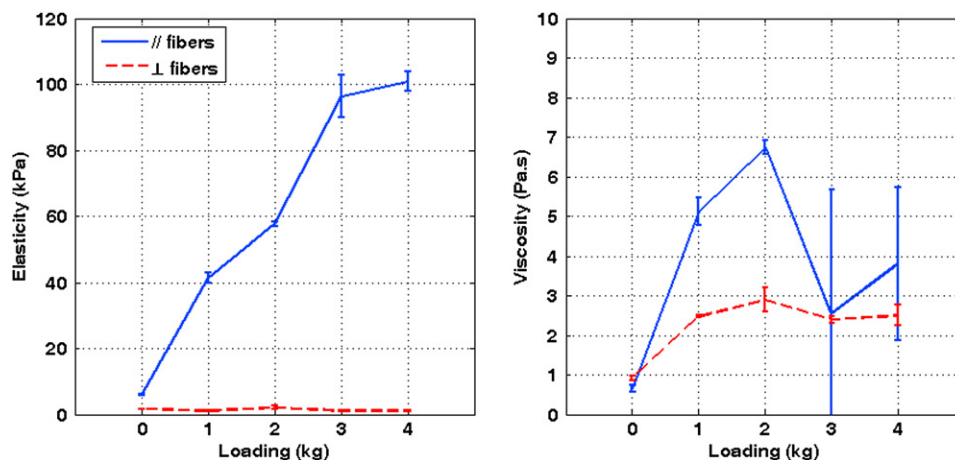


Fig. 8. Elasticity (μ) (a) and viscosity (η) (b) of the brachialis extracted from a Voigt's model using the dispersion measurement presented in Figure 7. Values are summarized in Table 1.

correspond to the mean velocity and to the standard deviation over these 3 mm² boxes. The shear wave mean group velocities over these ROIs increase faster along the fibers than perpendicularly to the muscle fibers while extending the elbow. Regarding the two different muscles, one can notice that the stretching does not have an impact on the elasticity of the superior muscle (biceps) but significantly on the antagonist muscle (brachialis).

Figure 11 is presented the shear modulus (μ) and viscosity (η) of the brachialis as a function of the passive extension of the elbow. Values are summarized in Table 3 correspond to dispersion measurements performed only in ROI no. 2.

DISCUSSION

This study represents a complete characterization of the mechanical parameters of the brachialis muscle *in vivo*. Using two different techniques for shear wave velocity assessment, two different approaches of the mechanical properties of muscle have been evaluated. First, group velocity estimation for the mapping of the shear wave velocity. Second, phase velocity estimation for SWS measurements for elasticity and viscosity quantification using a simple viscoelastic model. The

techniques were used for different configurations: contraction, stretching and anisotropy.

One interest of the SSI approach lies in the fact that it is weakly sensitive to motion artifacts, contrary to other radiation force imaging elastography techniques. This is due to the specificity of this technology that combines ultra-fast ultrasonic imaging and radiation force. Indeed, instead of repeating experiment stroboscopically several times to get a complete movie of the shear wave propagation over a large ROI, we acquire all data in one single ultra-fast sequence. Contrary to stroboscopic approaches, this genuine ultra-fast approach does not require concatenating acquisitions acquired at different times that are sensitive to motion artifacts. Second, tissue displacements are relative and estimated from one ultrasonic image to the next one. At a 2000 Hz frame rate, typical displacements induced using the radiation force are reaching 15 μ m from one ultrasonic image to the next one. In the experimental configuration, motion artifacts can easily be kept below 5 mm/s (relative speed between the array position and muscle tissues) corresponding to a 2.5 μ m displacement from one image to the other.

Regarding the contraction, the shear wave group velocity increases more significantly for each volunteer along the fibers rather than perpendicularly to the fibers.

Table 1. Elasticity and viscosity of the whole brachialis extracted from the dispersion curves using a Voigt's model as a function of the loading

Loading (kg)	0	1	2	3	4
Elasticity (kPa)					
//	5.86 ± 0.20	41.32 ± 1.86	57.58 ± 0.91	96.28 ± 7.13	100.80 ± 3.22
⊥	1.58 ± 0.15	1.07 ± 0.05	1.97 ± 0.52	1.12 ± 0.11	1.12 ± 0.21
Viscosity (Pa.s)					
//	0.65 ± 0.10	5.10 ± 0.38	6.72 ± 0.19	2.55 ± 3.50	3.80 ± 2.15
⊥	0.92 ± 0.06	2.47 ± 0.04	2.89 ± 0.33	2.39 ± 0.10	2.50 ± 0.29

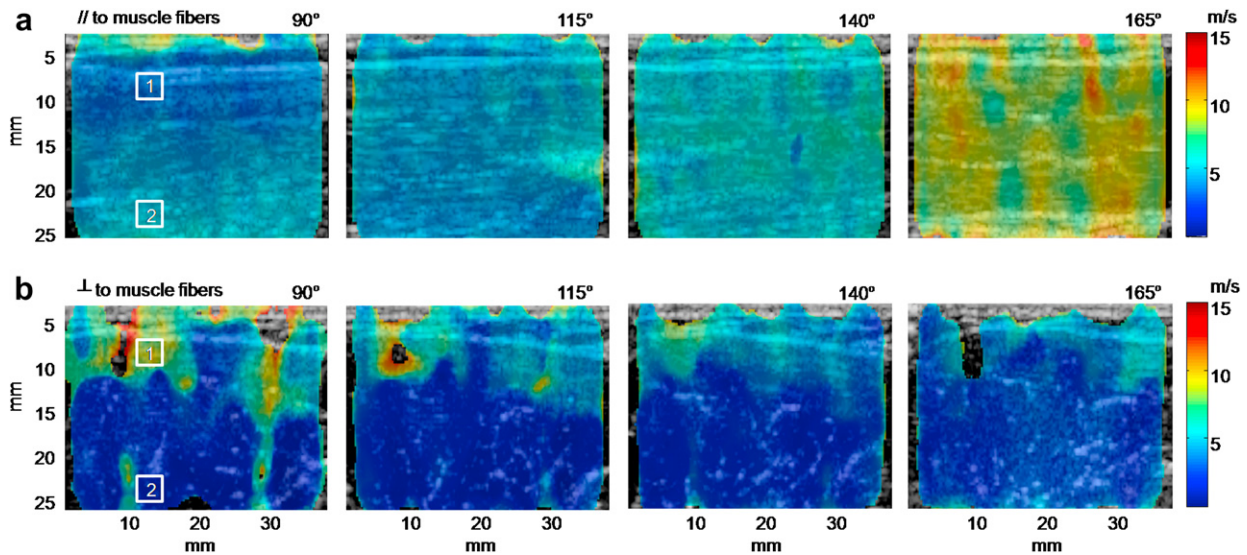


Fig. 9. Shear wave velocity maps of the biceps brachii for passive extension of the elbow with different angle (from 90° to 165° with 25° step) along the fibers (a) and perpendicularly to the fibers (b). The first ROI (3 mm^2 box) is chosen in the biceps muscle whereas the second one is in the brachialis.

In Figure 5 one can notice that the shear wave group velocity increases by about a factor 3 along the fibers and 1.5 perpendicularly to the fibers (which represents a factor of about 9 and 2.25 on shear modulus respectively). Such a difference results from the strong anisotropy of the muscle that is well known in biomechanics. Hence, the changes in transversal muscle hardness during contraction could be attributed to structural modifications. Namely, the progressive tension on myofilaments due to contractile protein longitudinal movement, leads to an increase in the transversal section and also to an increase in intra-muscular pressure as the muscle is placed in a closed volume (Fung 1981). Such a natural conception of the muscle leads to some strong anisotropic properties that are varying as a function of the contraction. In Figure 6, the shear wave group velocity in the brachialis for two different levels of loading is presented. The anisotropic ratio between rest and 3 kg loading increases strongly with the angle of propagation of shear wave with respect to the main muscular fibers axis. Compared with the acquisition performed in reference Gennisson et al. 2003, results are in the same order of magnitude.

In 2003, the acquisition was done on a slightly contracted muscle due to the experimental set-up. The position of the arm between the two experiments and the two subjects was different. In the 2003 article, the arm was vertical and the subject was contracting his muscle a little bit to facilitate the positioning of the shear elasticity probe. In this article, the arm rests horizontally without any contraction. Such set-up differences strongly affect estimates. The experimental set-up chosen in this article is much more adapted to muscle characterization as it enables to control the rest, the contraction and the positioning of the arm.

The SWS technique, which enables to measure the dispersion of shear wave *in vivo*, has been applied for diverse configurations on the same volunteer. The same behavior can be observed than for the group velocity mapping, namely the role of contraction on the shear velocity and the high anisotropy of the muscle. The SWS does not allow to produce maps but gives access in a ROI to the dispersion of the wave through the measurement of the phase velocity $v_\phi(\omega)$. The shear wave dispersion is related to the viscoelastic parameters

Table 2. Shear wave group velocity versus the elbow's angle for a passive extension, along (//) and perpendicularly (\perp) to the fibers in the biceps muscle and in the antagonist muscle.

Angle of the elbow φ ($^\circ$)	90°	115°	140°	165°
Shear wave group velocity (//) (m/s)				
ROI no. 1	2.73 ± 0.02	2.75 ± 0.03	3.93 ± 0.07	5.68 ± 0.03
ROI no. 2	3.11 ± 0.02	2.67 ± 0.02	4.09 ± 0.01	5.56 ± 0.09
Shear wave group velocity (\perp) (m/s)				
ROI no. 1	2.27 ± 0.05	2.15 ± 0.16	1.89 ± 0.05	2.48 ± 0.06
ROI no. 2	1.23 ± 0.10	1.15 ± 0.01	1.02 ± 0.02	1.78 ± 0.03

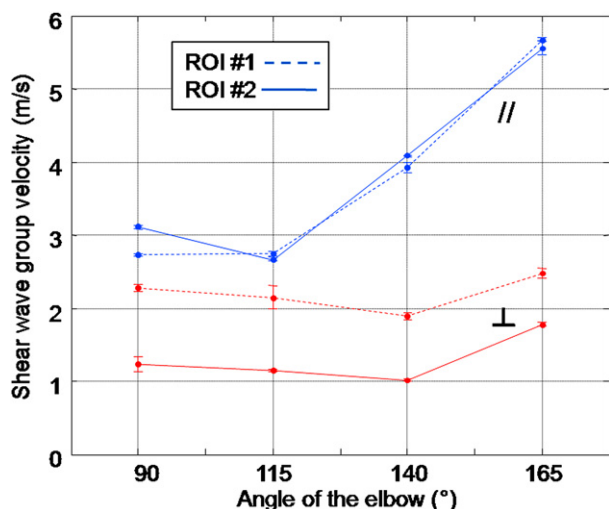


Fig. 10. Shear wave group velocity along the fibers and perpendicularly to the fibers in the two ROIs defined in Figure 11 as a function of the extension of the elbow. The two ROIs defined on the biceps brachii and on the brachialis are distinguishable only perpendicularly to the fibers.

of the medium through a rheologic model. It, thus, gives a more complete set of information on the tissue behavior than the simple mapping of the group velocity. Here, the Voigt’s model was chosen because it best describes many phantom gels and has been successfully applied to muscle tissue before (Catheline *et al.* 2004; Fung 1981). The Voigt model allows to compute both elasticity μ and viscosity η from either attenuation $\alpha(\omega)$ or phase velocity $v_\varphi(\omega)$ of a shear wave propagating in the medium. Here, the inversion of eqn (3) was done thanks to a Nelder-Mead nonlinear optimization technique that could probably be improved in future work to obtain

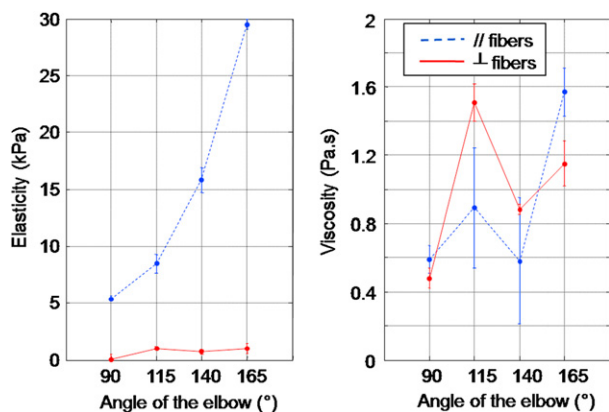


Fig. 11. Elasticity (μ) and viscosity (η) of the brachialis along (//) and perpendicularly (\perp) to the fibers as a function of the passive extension of the elbow extracted from a Voigt’s model using the dispersion measurement in ROI no. 2. For both cases, viscosity slightly increases whereas elasticity strongly increases along the fibers than perpendicularly to the fibers.

a higher stability and accuracy. As the attenuation $\alpha(\omega)$ was not measured here due to signal to noise ratio, the Voigt model was not validated on this particular dataset. It should, thus, be understood at this point as an hypothesis made on the tissue mechanical behavior. Future work would need to find a robust way to validate this model thanks to the reliable estimation of the attenuation. The analysis of the measured viscosity in terms of molecular cross bridging during the contraction process would also be of great interest.

As a function of the voluntary contraction of the muscle, both elasticity and viscosity increase along the fibers (Table 1), when perpendicularly to the fibers elasticity remains constant and viscosity increases. The elasticity increases by about a factor of 20 along the fibers and is constant perpendicularly to the fibers from 0 to 4 kg loading. Along the fibers, such elasticity increase is well known (Nordez *et al.* 2008; Genisson *et al.* 2003, 2005; Fung 1981) and the ratio of elasticity between rest and maximum contraction can be higher. In this article, the maximum contraction of each volunteer was not reached. Concerning viscosity, it increases by factor of about 10 along the fibers and 3 perpendicularly. These results are in good agreement with the literature where it is well known that viscosity increases with contraction (Desplantez *et al.* 1999; Martin *et al.* 1994). Nevertheless, the strong increase of viscosity along the fibers could also be explained by the use of Voigt’s model (Fung 1981; Kruse *et al.* 2000; Genisson *et al.* 2004), which is the simplest model usually applied for biologic tissues in which an increase of the speed of the shear wave leads to an increase of elasticity but also viscosity.

Regarding the muscle stretching without voluntary contraction, the SSI technique shows that it is able to differentiate muscles from the mapping of their elasticity changes during stretching. It clearly appears on elasticity images transversally to the fibers (Fig. 10) that brachialis and biceps are separable. Moreover, one can notice that the stretching impact principally along the fibers on elasticity (Fig. 11). Even if the slope of the viscosity with the angle of extension increases (in both cases, perpendicular and parallel to the fibers), no significant changes are noticeable. This could be explained simply by the composition of the muscle made up of hundreds of align fibers. No specific connections are present transversally between fibers (Fung 1981). Based on these results, we believe that the Supersonic Shear Imaging technique and the associated SWS technique are suitable to characterize the complexity of muscle tissue *in vivo* with little to no hassle. They might pave the way for lightweight clinical assessment of the viscoelastic parameters of muscle tissue.

The interest of assessing fully and quantitatively muscle tissue viscoelasticity lies mainly in monitoring

Table 3. Elasticity and viscosity in the brachialis as a function of the angle φ of the elbow for a passive extension along ($//$) and perpendicularly (\perp) to the fibers

Angle of the elbow φ ($^\circ$)	90 $^\circ$	115 $^\circ$	140 $^\circ$	165 $^\circ$
Elasticity (kPa)				
$//$	5.40 \pm 0.25	8.46 \pm 0.79	15.80 \pm 1.07	29.52 \pm 0.42
\perp	0.05 \pm 0.43	1.03 \pm 0.11	0.73 \pm 0.21	1.01 \pm 0.41
Viscosity (Pa.s)				
$//$	0.59 \pm 0.08	0.89 \pm 0.35	0.58 \pm 0.37	1.57 \pm 0.14
\perp	0.48 \pm 0.06	1.51 \pm 0.11	0.88 \pm 0.03	1.15 \pm 0.13

Values estimated using the Voigt's model.

neuromuscular diseases such as myopathies (as stated in the introduction, clinicians report a qualitative increase in hardness of muscles of myopathic people) and monitoring recovery after injury. Whereas a correlation between viscoelastic parameters can effectively be clinically proven remains an open question. We hope that this work can help set up a protocol and future clinical trials to help answer this question. It also emphasizes the need to control all parameters when measuring muscle mechanical properties and when developing muscle models. Hopefully, a better understanding of a simple skeletal muscle such as the biceps brachialis might give some insight for the most complex muscles such as the cardiac muscle where anisotropy, viscosity and passive stretching might also play an essential role but are far more difficult to assess *in vivo* independently.

CONCLUSION

A quantitative way to measure the complex viscoelastic parameters was investigated *in vivo* in healthy volunteers. It provides a first set of quantitative values for biomechanical properties of muscle perpendicularly and along the fibers. The estimation of shear modulus, shear viscosity and shear anisotropy and their respective changes during isometric contraction or passive extension was performed *in vivo* and provides a complete set of quantitative data. These data could benefit in a better understanding of muscle mechanics, provide quantitative values for biomechanical models and simulations, and finally describe quantitatively the normal characteristics of muscle in healthy volunteers for further comparisons with pathological states. Clinical validation of elastography techniques for diagnosis and monitoring of neuromuscular diseases or recovery will need to inspect the full scope of these parameters in order to produce reliable and precise results. Finally, one can hope that this stunning complexity of the muscle tissue will not simply be a drawback for elastography techniques but can also turn into a more powerful way to reveal the muscle state and a powerful screening tool.

Acknowledgements—The authors would like to thank Benoit Larrat and Gianmarco Pinton for their assistance.

REFERENCES

- Aminoff MJ. Electromyography in clinical practice. 3rd ed. New-York: Churchill Livingstone; 1987.
- Bercoff J, Tanter M, Fink M. Supersonic shear imaging: A new technique for soft tissues elasticity mapping. *IEEE Trans Ultrason Ferroelectr Freq Control* 2004;51:396–409.
- Catheline S, Gennisson JL, Delon G, Sinkus R, Fink M, Abouelkaram S, Culioli J. Measurement of viscoelastic properties of homogeneous soft solid using transient elastography: An inverse problem approach. *J Acoust Soc Am* 2004;116:3734–3741.
- Chen S, Fatemi M, Greenleaf JF. Quantifying elasticity and viscosity from measurement of shear wave speed dispersion. *J Acoust Soc Am* 2004;115:2781–2785.
- Deffieux T, Gennisson JL, Tanter M, Fink M. Assessment of the mechanical properties of musculoskeletal system using 2D and 3D very high frame rate ultrasound. *IEEE Trans Ultrason Ferroelectr Freq Control* 2008;55:2177–2190.
- Deffieux T, Montaldo G, Tanter M, Fink M. Shear wave spectroscopy for *in vivo* quantification of human soft tissues viscoelasticity. *IEEE Trans Med Imaging* 2009;28:313–322.
- Desplantez A, Cornu A, Goubel F. Viscous properties of human muscle during contraction. *J Biol* 1999;32:555–562.
- Dresner MA, Rose GH, Rossman PJ, Muthupillai R, Manduca A, Ehman RL. Magnetic resonance elastography of skeletal muscle. *J Magn Reson Imaging* 2001;13:269–276.
- Fung YC. Biomechanics: Mechanical properties of living tissues. 2nd edition. New York: Springer; 1981.
- Gennisson JL, Catheline S, Chaffai S, Fink M. Transient elastography in anisotropic medium: Application to the measurement of slow and fast shear waves velocities in muscles. *J Acoust Soc Am* 2003;114:536–541.
- Gennisson JL, Cornu C, Catheline S, Fink M, Portero P. Human muscle hardness assessment during incremental isometric contraction using transient elastography. *J Biol* 2005;38:1543–1550.
- Kruse S, Smith J, Lawrence A, Dresner M, Manduca A, Greenleaf J, Ehman R. Tissue characterization using magnetic resonance elastography: Preliminary result. *Phys Med Biol* 2000;45:1579–1590.
- Martin A, Martin L, Morlon B. Theoretical and experimental behavior of the muscle viscosity coefficient during maximal concentric actions. *Eur J Appl Physiol* 1994;69:539–544.
- Nelder J, Mead R. A simplex method for function minimization. *Computer Journal* 1965;7:308–313.
- Nordez A, Gennisson JL, Casari P, Catheline S, Cornu C. Characterization of muscle belly elastic properties during passive stretching using transient elastography. *J Biomech* 2008;41:2305–2311.
- Orizio C. Muscle sound: Bases for the introduction of a mechanomyographic signal in muscle studies. *Crit Rev Biol Eng* 1993;21:201–243.
- Papazoglou S, Braun J, Hamhaber U, Sack I. Two-dimensional wave-form analysis in MR elastography of skeletal muscles. *Phys Med Biol* 2005;50:1313–1325.

- Paris D, Paris F. Passive stiffness is increased in soleus muscle of desmin knockout mouse. *Muscle Nerve* 2001;24:1090–1092.
- Ringleb SI, Bensamoun SF, Chen Q, Manduca A, An KN, Ehman RL. Applications of magnetic resonance elastography to healthy and pathologic skeletal muscle. *J Magn Reson Imaging* 2007;25:301–309.
- Royer D, Dieulesaint E. *Elastic waves in solid*. Vol. 1. Berlin: Springer Verlag; 1996.
- Tanter M, Bercoff J, Athanasiou A, Deffieux T, Gennisson JL, Montaldo G, Tardivon A, Fink M. Quantitative assessment of breast lesions viscoelasticity using supersonic shear imaging technique: Initial clinical investigation. *Ultrasound Med Biol* 2008;34:1373–1386.
- Viby-Mogensen J, Jensen E, Werner M, Kirkegaard H. Measurement of acceleration: A new method of monitoring neuromuscular function. *J Clin Anaesth* 2003;15:145–148.
- Zimmer JE, Cost JR. Determination of the elastic constants of an unidirectional fiber composite using ultrasonic velocity measurements. *J Acoust Soc Am* 1970;47:795–803.